Biochemistry and Biophysics Reports 28 (2021) 101167

Contents lists available at ScienceDirect

Biochemistry and Biophysics Reports

journal homepage: www.elsevier.com/locate/bbrep

Two distinct phenotypes of immunologically hot gastric cancer subtypes

Noriyuki Saito [a], Yukari Kobayashi [b], Koji Nagaoka [b], Yoshihiro Kushihara [b], Yasuyoshi Sato [c], Ikuo Wada [d], Kazuhiro Kakimi [b,*], Yasuyuki Seto [a]

[a] Department of Gastrointestinal Surgery, The University of Tokyo Graduate School of Medicine, Tokyo 113-8655, Japan
[b] Department of Immunotherapeutics, The University of Tokyo Hospital, Tokyo 113-8655, Japan
[c] Department of Medical Oncology, The Cancer Institute Hospital of Japanese Foundation for Cancer Research, Tokyo 135-8550, Japan
[d] Department of Surgery, Tokyo Metropolitan Bokutoh Hospital, Tokyo 130-8575, Japan

ARTICLE INFO

Keywords:
Gastric cancer
Tumor immunity
RNA-Seq
T cell-inflamed
Hot tumor

ABSTRACT

An in-depth understanding of the tumor microenvironment (TME) is required for the development of improved combination immunotherapies for gastric cancer. Recently, we classified these cancers into four main types defined by their immunological attributes, namely Hot 1, Hot 2, Intermediate and Cold. Of these, the T cell-inflamed "Hot" tumors were further divided into Hot 1 and Hot 2 with different clinical outcomes. Thus, overall survival and progression-free survival of patients with Hot 1 tumors were shorter than with Hot 2. In the present study, we re-evaluated RNA-Seq data of 6 Hot 1 and 6 Hot 2 gastric cancers to elucidate the underlying reason for the poor prognosis and T cell dysfunction in the former. In addition, 56 Hot 1 and 27 Hot 2 tumors in The Cancer Genome Atlas (TCGA) were analyzed. We report that single sample Gene Set Enrichment Analysis (ssGSEA) and differential gene expression analysis identified differences between Hot 1 and Hot 2 tumors involved in metabolism and cell adhesion pathways. Therefore, it is suggested that strategies to modulate active metabolism in Hot 1 tumors should be integrated into the treatment of these gastric cancers.

1. Introduction

The prognosis of locally advanced and metastatic gastric cancers remains poor, making these tumors the world's fourth leading cause of cancer death [1]. Immune checkpoint inhibitors (ICIs) targeting the PD-1/PD-L1 pathway were approved for the treatment of gastric cancer in 2017. Although they improved the prognosis of this disease, only a small proportion of patients benefit from ICI [2,3]. Different treatment strategies such as earlier use or combination with chemotherapy are being investigated in an effort to overcome this limitation [4,5].

A better understanding of antitumor immunity will help predict the prognosis of gastric cancer patients and customize the appropriate therapies in each patient. Therefore, immune profiling of gastric cancer and immunological classification were extensively studied [6–9]. Previously, we also proposed a novel immunological classification of gastric cancer [10]. We performed RNA-Seq and analyzed the tumor microenvironment (TME) of gastric cancer in the context of the so-called "cancer-immune cycle" [11]. We then proposed an "Immunogram Score" classification for gastric cancer [10]. According to this, gastric cancers were immunologically classified into several types, designated Hot, Intermediate and Cold. T cell-inflamed Hot tumors were further divided into Hot 1 and Hot 2 tumors. The former is characterized by exhibiting an activated glycolysis signature and by more intra-tumoral $CD8^+$ T cell infiltration than the latter. Surprisingly, however, both overall survival (OS) and progression-free survival (PFS) of patients with Hot 1 tumors were worse than for Hot 2 tumors, possibly due to profound T cell dysfunction in the former determined by the expression of checkpoint molecules and impaired cytokine production in ex vivo tumor-infiltrating lymphocyte using flow cytometry.

Novel combination immunotherapy for patients with Hot 1 tumors must be developed, bearing these characteristics in mind. Among 29 RNA-Seq data in our previous study [10], we focused on 12 RNA-Seq data of patients who were classified in Hot 1 or Hot 2 subtype. We newly re-evaluated the RNA-Seq data of Hot 1 and Hot 2 tumors of same patients to understand the underlying reasons for the poor prognosis of Hot 1 tumors and whether this was indeed associated with T cell dysfunction.

* Corresponding author. The University of Tokyo Hospital, 7-3-1 Hongo, Bunkyo-ku, Tokyo, 113-8655, Japan.
E-mail address: kakimi@m.u-tokyo.ac.jp (K. Kakimi).

https://doi.org/10.1016/j.bbrep.2021.101167
Received 5 October 2021; Received in revised form 28 October 2021; Accepted 30 October 2021

Abbreviations

ICI	immune checkpoint inhibitor
TME	tumor microenvironment
OS	overall survival
PFS	progression free survival
HER2	human epidermal growth factor receptor 2
TCGA	The Cancer Genome Atlas
ssGSEA	single sample Gene Set Enrichment Analysis
GO	Gene Ontology
MSigDB	Molecular Signatures Database
DEG	Differentially Expressed Gene
IPA	Ingenuity Pathway Analysis
EMT	epithelial-to-mesenchymal transition
MSI	microsatellite instability
EBV	Epstein-Bar virus
GS	genomically stable
CIN	chromosomal instability

2. Materials and methods

2.1. Patients and data sets

Complete immune profiling was performed on 29 patients diagnosed with histologically-confirmed gastric cancer at Tokyo Metropolitan Bokutoh Hospital between June 2014 and October 2017, designated the "BKT cohort" [10]. Clinical profiles with histology by the Lauren classification, macroscopic classification by the Borrmann classification, locus of the primary site, TNM clinical staging, overexpression of human epidermal growth factor receptor 2 (HER2) protein and the presence or absence of Helicobacter pylori infection were reported in our previous work [10]. These patients' tumors were immunologically classified into Hot 1, Hot 2, Intermediate and Cold subtypes. We have now re-analyzed the transcriptomic data of 6 of each of the Hot subtypes. All procedures were performed following the ethical standards of the participating institutions and in conformity with the 1964 Declaration of Helsinki and its later amendments or comparable ethical standards. Informed written consent was obtained from all patients included in the study, which was approved by the Research Ethics Committees of the University of Tokyo (No. G3545) and Tokyo Metropolitan Bokutoh Hospital (No. 25-38-02). In addition, the TCGA cohort (https://portal.gdc.cancer.gov/) was also investigated for the 56 Hot 1 and 27 Hot 2 tumors previously identified [10]. A summary of patients' characteristics is provided in Supplementary Table S1.

2.2. Transcriptomics

In the previous study, RNA-Seq of bulk tumor tissue was performed [10]. RNA-Seq data of BKT patients are available at DDBJ Sequence Read Archive (Accession no. DRA009379) [10]. Independent to our previous study, RNA-Seq data were subjected to single sample Gene Set Enrichment Analysis (ssGSEA) using gene sets of Hallmark and Gene Ontology (GO) Biological Process ontology registered in the Molecular Signatures Database (MSigDB, https://www.gsea-msigdb.org/gsea/msigdb/). The enrichment score is obtained using the ssGSEA method with R package ssGSEA 2.0 (https://github.com/broadinstitute/ssGSEA2.0) and R software version 3.6.0. The TCC-GUI (Graphical User Interface for TCC package, https://infinityloop.shinyapps.io/TCC-GUI/) was used to investigate differentially expressed genes (DEGs) between Hot 1 and Hot 2 tumors. DESeq2 was selected for normalization and DEG identification [12]. Genes with the $\log_2$ fold-change greater than 1 and adjusted p-value smaller than 0.05 were selected as DEGs. The DEGs from TCC-GUI (M-value<-1 or >1 and p-value<0.05) were submitted to the Ingenuity Pathway Analysis (IPA, QIAGEN, Redwood City, CA, USA) software. Canonical pathways, upstream regulators, regulator effects, diseases and biological functions were analyzed. Using machine learning techniques, a graphical summary was depicted.

2.3. Statistical analyses

The ssGSEA scores were compared between the two groups by Wilcoxon's test. For categorical variables, Fisher's exact test or the chi-square test was used. JMP Pro 15 (SAS Institute Japan, Tokyo, Japan) was used for statistical analysis. A value of $p < 0.05$ was considered statistically significant.

3. Results

3.1. Patients' characteristics

Patients' characteristics are shown in Table 1. There were no significant differences between the Hot 1 and Hot 2 groups in terms of clinicopathological features. However, 4 of 6 tumors in the Hot 1 group

Table 1
Clinicopathological characteristics.

	BKT			TCGA		
	Hot 1 (n = 6)	Hot 2 (n = 6)	p-value	Hot 1 (n = 56)	Hot 2 (n = 27)	p-value
Age (years), mean ± SD	73.2 ± 3.2	66.0 ± 3.2	0.15	67.3 ± 1.6	62.7 ± 2.2	0.10
Sex, n						
Male/Female	4/2	6/0	0.45	30/26	14/13	0.88
Locus, n						
GE/U/M/L	1/0/2/3	0/2/1/3	0.55			
Macroscopic type (Borrmann), n						
1/2/3/4/5	0/3/3/0/0	1/3/1/0/1	0.55			
pStage, n						
I/II/III/IV/not reported	1/1/3/1/0	1/3/2/0/0	0.74	6/17/22/7/4	2/5/18/1/1	0.21
Histology (Differentiation), n						
differentiated/undifferentiated	0/6	3/3	0.18			
Histology (Lauren classification), n						
intestinal/diffuse/mixed/indeterminant	3/0/3/0	5/0/1/0	0.55			
HER2 status, n						
positive/negative	1/5	1/5	1			
Helicobacter pylori infection, n						
positive/negative/not reported	5/1/0	3/3/0	0.54	4/17/35	1/10/16	0.46
Molecular classification by TCGA, n						
MSI/EBV/GS/CIN	4/0/0/2	1/3/0/2	0.13	26/9/1/20	2/12/3/10	0.0006
Mesenchymal subtype by ACRG, n						
Mesenchymal/Non-mesenchymal	0/6	2/4	0.45			

MSI: microsatellite instability, EBV: Epstein-Bar virus, GS: genomically stable, CIN: chromosomal instability.

were of the MSI subtype according to the TCGA molecular classification, while 3 of the 6 in the Hot 2 group were classified as EBV subtype ($p = 0.13$, not statistically significant). This tendency is consistent with the TCGA cohort data where the MSI subtype was significantly more frequent in the 56 Hot 1 tumors, but the EBV subtype was more common in among the 27 Hot 2 tumors ($p = 0.0006$).

3.2. Gene enrichment and pathway analysis

As a starting point, ssGSEA analysis with all 50 hallmark gene sets was performed to compare Hot 1 and Hot 2 patients (Table 2, Supplementary Table S2). Of these 50, upregulation only of the 3 gene set signatures HALLMARK UV response ($p = 0.0306$), HALLMARK cholesterol homeostasis ($p = 0.0453$) and HALLMARK glycolysis ($p = 0.0082$) were detected in Hot 1 tumors. DEGs between Hot 1 and Hot 2 tumors were identified by TCC-GUI and are visualized in Fig. 1A as a volcano plot. Up-regulated genes in Hot 1 and Hot 2 tumors are listed in Supplementary Table S3; these amounted to 103 and 205 genes in Hot 1 and Hot 2 tumors, respectively. Genes related to the cytoskeleton and cell adhesion, such as DSG3, DSC2, SCEL, KRT16, and GJB7, were up-regulated in Hot 1 tumors. The DEGs and corresponding p-values were subjected to Causal Network Analysis on the IPA platform and a summary of the results is given in Fig. 1B. This highlights CDH1 and NEUROG1 in Hot 1 tumors.

3.3. Validation of gene enrichment results

Based on the global analysis using ssGSEA with hallmark gene sets and the DEG analysis, Hot 1 tumors were proposed to be metabolically active and enriched for cellular components. To confirm these results, additional gene sets related to these two categories were extracted from GO Biological Process ontology gene sets and used to compare Hot 1 with Hot 2 tumors (Supplementary Table S4). As shown in Table 3, several gene sets associated with cellular components and metabolism were enriched in Hot 1 tumors. The cellular component-related gene sets included apical junction assembly ($p = 0.0306$), cell cell junction

Table 2
Comparison between Hot 1 and Hot 2 tumors by ssGSEA with hallmark gene sets.

Hallmark	Process Category	Hot 1 (n = 6)	Hot 2 (n = 6)	p-value	Upregulated in
HM_APICAL_SURFACE	cellular component	2640.0 ± 630.3	2475.6 ± 1421.8	0.9362	N·S.
HM_APICAL_JUNCTION	cellular component	5260.5 ± 387.0	5035.0 ± 845.2	1	N·S.
HM_PEROXISOME	cellular component	5625.7 ± 629.8	5437.3 ± 471.3	0.6889	N·S.
HM_ANGIOGENESIS	development	5853.8 ± 773.2	6710.6 ± 1599.3	0.4712	N·S.
HM_PANCREAS_BETA_CELLS	development	−570.6 ± 690.6	−394.5 ± 1018.3	0.8102	N·S.
HM_EPITHELIAL_MESENCHYMAL_TRANSITION	development	5702.2 ± 754.6	6540.5 ± 1592.6	0.4712	N·S.
HM_SPERMATOGENESIS	development	−1759.1 ± 619.1	−2172.0 ± 377.2	0.1735	N·S.
HM_MYOGENESIS	development	2140.9 ± 626.6	2812.4 ± 1769.2	0.2298	N·S.
HM_ADIPOGENESIS	development	6727.5 ± 457.3	6412.8 ± 288.5	0.298	N·S.
HM_DNA_REPAIR	DNA damage	6623.2 ± 382.5	6356.8 ± 397.8	0.298	N·S.
HM_UV_RESPONSE_DN	DNA damage	3505.6 ± 510.5	4188.1 ± 1302.7	0.3785	N·S.
HM_UV_RESPONSE_UP	DNA damage	6404.9 ± 170.2	6067.6 ± 304.3	0.0306	Hot 1
HM_COAGULATION	immune	4659.0 ± 709.6	5638.2 ± 905.9	0.1735	N·S.
HM_ALLOGRAFT_REJECTION	immune	7072.8 ± 825.7	7621.0 ± 387.6	0.4712	N·S.
HM_COMPLEMENT	immune	6115.7 ± 651.3	6483.8 ± 802.7	0.3785	N·S.
HM_INFLAMMATORY_RESPONSE	immune	4238.7 ± 1077.8	5037.6 ± 920.5	0.2298	N·S.
HM_INTERFERON_GAMMA_RESPONSE	immune	7865.0 ± 828.5	8190.8 ± 380.9	0.6889	N·S.
HM_INTERFERON_ALPHA_RESPONSE	immune	8597.0 ± 606.2	8714.1 ± 299.7	0.9362	N·S.
HM_IL6_JAK_STAT3_SIGNALING	immune	5566.0 ± 1178.1	6254.6 ± 842.0	0.3785	N·S.
HM_BILE_ACID_METABOLISM	metabolic	1855.5 ± 1215.0	1636.0 ± 794.9	0.6889	N·S.
HM_FATTY_ACID_METABOLISM	metabolic	6137.7 ± 574.3	5824.2 ± 476.5	0.4712	N·S.
HM_XENOBIOTIC_METABOLISM	metabolic	4228.0 ± 469.3	4383.6 ± 412.9	0.5752	N·S.
HM_HEME_METABOLISM	metabolic	3802.4 ± 286.7	3392.2 ± 391.9	0.1282	N·S.
HM_OXIDATIVE_PHOSPHORYLATION	metabolic	8401.4 ± 318.1	8053.9 ± 336.9	0.0927	N·S.
HM_CHOLESTEROL_HOMEOSTASIS	metabolic	7228.5 ± 262.1	6846.1 ± 309.6	0.0453	Hot 1
HM_GLYCOLYSIS	metabolic	6108.7 ± 365.1	5363.8 ± 376.8	0.0082	Hot 1
HM_UNFOLDED_PROTEIN_RESPONSE	pathway	7808.1 ± 181.3	7720.1 ± 303.9	0.6889	N·S.
HM_REACTIVE_OXYGEN_SPECIES_PATHWAY	pathway	8666.6 ± 63.3	8589.4 ± 256.7	0.298	N·S.
HM_PROTEIN_SECRETION	pathway	7136.2 ± 275.8	6676.0 ± 441.3	0.0656	N·S.
HM_APOPTOSIS	pathway	7235.5 ± 318.3	7414.8 ± 553.3	0.3785	N·S.
HM_HYPOXIA	pathway	5757.9 ± 311.8	5665.5 ± 949.8	0.9362	N·S.
HM_P53_PATHWAY	proliferation	6944.5 ± 453.1	6759.0 ± 265.1	0.4712	N·S.
HM_MYC_TARGETS_V2	proliferation	7407.7 ± 473.6	6720.1 ± 1245.1	0.3785	N·S.
HM_MYC_TARGETS_V1	proliferation	9032.5 ± 75.5	8942.1 ± 209.5	0.6889	N·S.
HM_MITOTIC_SPINDLE	proliferation	4886.7 ± 343.9	4667.2 ± 579.8	0.8102	N·S.
HM_G2M_CHECKPOINT	proliferation	6344.7 ± 596.7	5868.5 ± 835.6	0.5752	N·S.
HM_E2F_TARGETS	proliferation	6696.0 ± 532.6	6207.4 ± 921.5	0.298	N·S.
HM_ESTROGEN_RESPONSE_EARLY	signaling	4508.9 ± 748.9	3720.7 ± 926.8	0.298	N·S.
HM_KRAS_SIGNALING_DN	signaling	−2923.5 ± 1004.4	−3111.7 ± 1277.2	0.2298	N·S.
HM_KRAS_SIGNALING_UP	signaling	3768.6 ± 956.9	4262.3 ± 1071.2	0.4712	N·S.
HM_ANDROGEN_RESPONSE	signaling	6895.2 ± 217.5	6882.0 ± 574.0	0.3785	N·S.
HM_TNFA_SIGNALING_VIA_NFKB	signaling	6268.1 ± 1040.1	6905.1 ± 679.6	0.298	N·S.
HM_IL2_STAT5_SIGNALING	signaling	4864.5 ± 624.7	5138.0 ± 546.3	0.8102	N·S.
HM_NOTCH_SIGNALING	signaling	4008.7 ± 316.7	4274.5 ± 788.8	0.4712	N·S.
HM_TGF_BETA_SIGNALING	signaling	6478.6 ± 536.3	6903.3 ± 523.3	0.1735	N·S.
HM_HEDGEHOG_SIGNALING	signaling	105.5 ± 643.3	1067.6 ± 1529.6	0.1735	N·S.
HM_PI3K_AKT_MTOR_SIGNALING	signaling	6613.1 ± 195.1	6400.0 ± 527.2	0.4712	N·S.
HM_WNT_BETA_CATENIN_SIGNALING	signaling	2396.2 ± 611.1	2530.4 ± 1345.6	0.8102	N·S.
HM_ESTROGEN_RESPONSE_LATE	signaling	5253.4 ± 608.3	4613.3 ± 962.9	0.1282	N·S.
HM_MTORC1_SIGNALING	signaling	7856.3 ± 104.9	7592.0 ± 288.7	0.2298	N·S.

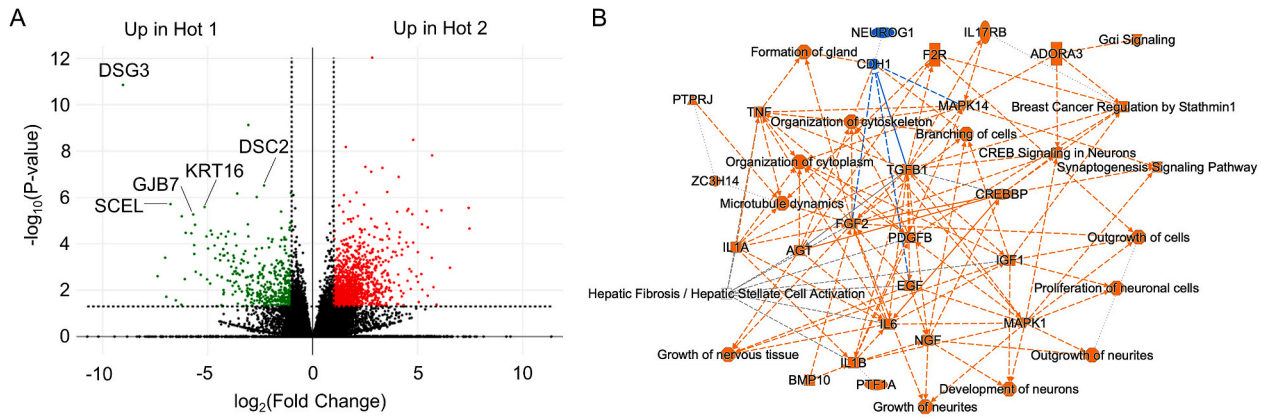

Fig. 1. Differentially expressed genes in Hot 1 and Hot 2 gastric cancer. (A) Volcano plot showing differentially expressed genes in Hot 1 and Hot 2 tumors. Fold-changes (x-axis) and statistical significance (-log10 of p-value, y-axis) are displayed as a dashed line where p = 0.05 and fold-change = 2 (log2 = 1). (B) Graphical summary of IPA.

organization (p = 0.0453), desmosome organization (p = 0.0306), hemidesmosome assembly (p = 0.0306), tight junction organization (p = 0.0306), intermediate filament based process (p = 0.0453), and microvillus organization (p = 0.0306). Gene sets associated with metabolism included glucose-6-phosphate metabolic process (p = 0.0453), pyruvate metabolic process (p = 0.0131), positive regulation of fatty acid transport (p = 0.0202), regulation of mitochondrial outer membrane permeabilization involved in apoptotic signaling pathway (p = 0.0453), positive regulation of oxidative phosphorylation (p = 0.0453), ADP metabolic process (p = 0.0453), ATP metabolic process (p = 0.0306), NAD metabolic process (p = 0.0306), and NADH metabolic process (p = 0.0306). To validate these results, RNA-Seq data of Hot 1 and Hot 2 tumors in the TCGA cohort were also subjected to ssGSEA (Supplementary Table S5). The ssGSEA scores of the metabolic and cellular components that were increased in the Hot 1 tumors of the BKT cohort were also significantly increased in Hot 1 tumors of the independent TCGA dataset (Table 3).

4. Discussion

Following our previous work showing that T cell inflamed gastric cancers could be further classified into two subtypes designed Hot 1 and Hot 2 [10], here we more closely examined the difference between these tumors in an attempt to gain some understanding of the underlying mechanisms responsible for the poor prognosis of the former. We newly re-analyzed RNA-Seq data by ssGSEA and DEG analysis and Hot 1 tumors were found to be enriched for the expression of genes associated with cell junctions and cellular metabolism.

In our previous studies, Hot 1 tumors were distinguished from Hot 2 tumors by their enhanced glycolysis. The current study found that the active metabolic environment in Hot 1 tumors included enhanced lipid metabolism, oxidative phosphorylation and mitochondrial energy production, in addition to glycolysis. Thus, active metabolism in Hot 1 tumors might be one of the reasons for T cell dysfunction via increased competition with effector T cells [13]. Therefore, targeting and controlling activated glycolysis, lipid metabolism, oxidative phosphorylation and mitochondrial function in Hot 1 tumors would be expected to improve the antitumor T cell response, and hence prognosis [14–16].

In general, tumor cells gain mobility and invasiveness through the epithelial-to-mesenchymal transition (EMT) [17]. E-cadherin is a cell-adhesion factor responsible for maintaining adhesive intercellular junctions between epithelial cells and for controlling cellular polarity. In this manner, E-cadherin restricts cell migration and suppresses metastasis [18]. In gastric cancer, loss of function of adhesive factors such as CDH1 is reported to contribute to tumor progression and metastasis [19]. Thus, the fact that the expression of CDH1, the E-cadherin gene, was identified as a factor strongly associated with the poor prognosis of patients in the Hot 1 group (Fig. 1B) seems inconsistent with this report. On the other hand, there is also a report that E-cadherin expression facilitates tumor growth and metastasis formation in breast cancer [20], which might be involved in the progression and poor prognosis of Hot 1 tumors, but not necessarily other gastric cancer subtypes or other cancer entities. Currently, several E-cadherin activators that restore their expression are expected to inhibit EMT and metastasis [19]. However, the pro-metastatic or anti-metastatic function of E-cadherin is likely to be highly context-dependent. As we showed in this study, E-cadherin activator might be deleterious in Hot 1 patients.

There are several limitations to this study. First, we collected the surgical specimens from a single institution. The small total number of 12 patients conceivably led to a selection bias. We accessed RNA-Seq data from the TCGA database for use as a validation cohort to overcome this limitation. Second, the RNA-Seq data used in the present study was obtained from bulk tumors and contained RNAs from tumor cells, immune cells, stromal cells and other cell types. They do not provide information on their cellular composition. Although several computational tools were developed [21], it is difficult to determine which cells are responsible for the expression of the identified up- and down-regulated genes in the TME. Single-cell RNA-Seq analysis, immunohistochemistry and flow cytometry will be needed to clarify interactions between these cells. Finally, our results of bioinformatics analysis were not supported by verification of the results of patient samples, cell or animal models. The verification of the results is required in future analysis.

5. Conclusions

Comprehensive transcriptomic analysis revealed differences in metabolism and cell adhesion pathways between Hot 1 and Hot 2 tumors. Therefore, it is proposed that strategies to modulate active metabolism in Hot 1 tumors should be integrated into the treatment of Hot 1 gastric cancers.

Funding

This work was supported in part by JSPS KAKENHI Grant Number 20K09161. This study was also supported in part by AMED under Grant Number JP 19cm0106552 and JP 21ck0106639. The funder had no role in study design, data collection and analysis, interpretation, decision to

Table 3
Comparison between Hot 1 and Hot 2 tumors by ssGSEA with GO Biological Process ontology gene sets.

GO_Bio Precess	Process Category	BKT			TCGA		
		Hot 1 (n=6)	Hot 2 (n=6)	p-value	Hot 1 (n=56)	Hot 2 (n=27)	p-value
GO_APICAL_JUNCTION_ASSEMBLY	cellular component	5108.4 ± 158.5	4068.7 ± 736.4	0.0306	23965.2 ± 359.2	23496.1 ± 631.0	0.0005
GO_CELL_CELL_JUNCTION_ORGANIZATION	cellular component	3298.1 ± 238.9	2475.7 ± 573.4	0.0453	22713.9 ± 505.8	22246.2 ± 708.7	0.0016
GO_DESMOSOME_ORGANIZATION	cellular component	6905.8 ± 844.0	4441.1 ± 2575.4	0.0306	26765.4 ± 473.1	25690.6 ± 1496.3	<0.0001
GO_HEMIDESMOSOME_ASSEMBLY	cellular component	5936.9 ± 1517.7	3714.5 ± 1158.1	0.0306	26197.0 ± 1264.8	24558.4 ± 2396.8	0.0027
GO_TIGHT_JUNCTION_ORGANIZATION	cellular component	4512.9 ± 381.2	3000.8 ± 1014.1	0.0306	24317.9 ± 384.0	23858.2 ± 651.4	0.001
GO_INTERMEDIATE_FILAMENT_BASED_PROCESS	cellular component	2244.6 ± 1161.0	719.9 ± 1061.8	0.0453	19402.6 ± 1494.3	17742.7 ± 1390.0	<0.0001
GO_MICROVILLUS_ORGANIZATION	cellular component	6198.2 ± 903.1	4349.1 ± 1127.8	0.0306	23581.1 ± 706.1	22826.0 ± 1086.7	0.0025
GO_GLUCOSE_6_PHOSPHATE_METABOLIC_PROCESS	metabolic	5220.0 ± 675.7	4443.8 ± 391.6	0.0453	24510.9 ± 691.9	23736.1 ± 843.6	0.0002
GO_PYRUVATE_METABOLIC_PROCESS	metabolic	5270.1 ± 421.5	4401.7 ± 456.5	0.0131	22653.8 ± 514.0	22242.6 ± 557.8	0.0016
GO_POSITIVE_REGULATION_OF_FATTY_ACID_ TRANSPORT	metabolic	−472.0 ± 444.9	−1789.4 ± 847.3	0.0202	17586.8 ± 1473.3	16741.0 ± 1337.3	0.0107
GO_REGULATION_OF_MITOCHONDRIAL_OUTER _MEMBRANE_PERMEABILIZATION_INVOLVED_IN_APOPTOTIC_SIGNALING_PATHWAY	metabolic	7600.2 ± 305.1	7083.9 ± 384.8	0.0453	26047.5 ± 296.1	25814.7 ± 320.0	0.0014
GO_POSITIVE_REGULATION_OF_OXIDATIVE_PH OSPHORYLATION	metabolic	6667.6 ± 180.7	6128.4 ± 375.4	0.0453	24396.9 ± 1390.8	23532.1 ± 1708.9	0.0306
GO_ADP_METABOLIC_PROCESS	metabolic	5258.4 ± 473.5	4548.1 ± 513.3	0.0453	22644.8 ± 529.3	22328.8 ± 569.7	0.0157
GO_ATP_METABOLIC_PROCESS	metabolic	6858.6 ± 377.5	6419.6 ± 296.2	0.0306	24460.9 ± 383.9	24232.2 ± 365.0	0.011
GO_NAD_METABOLIC_PROCESS	metabolic	6930.7 ± 412.3	6193.4 ± 474.1	0.0306	22809.6 ± 629.9	22370.2 ± 632.7	0.006
GO_NADH_METABOLIC_PROCESS	metabolic	7310.2 ± 308.4	6700.0 ± 409.8	0.0306	23384.1 ± 718.0	22995.8 ± 672.7	0.0244

publish or preparation of the manuscript, or any aspect of the study.

Data repository and accession numbers

Data are deposited on DDBJ Sequence Read Archive (Accession no. DRA009379).

Declaration of competing interest

The authors declare the following financial interests/personal relationships which may be considered as potential competing interests:

Kazuhiro Kakimi reports a relationship with Takara Bio Inc that includes: funding grants. The Department of Immunotherapeutics, The University of Tokyo Hospital, is an endowed department by TAKARA BIO Inc.

Data availability

Data will be made available on request.

Acknowledgments

The authors thank Mikiko Shibuya, Yaeko Furuhashi, Yuki Yoshikawa for excellent technical assistance.

Appendix A. Supplementary data

Supplementary data to this article can be found online at https://doi.org/10.1016/j.bbrep.2021.101167.

References

[1] H. Sung, J. Ferlay, R.L. Siegel, M. Laversanne, I. Soerjomataram, A. Jemal, F. Bray, Global cancer statistics 2020: GLOBOCAN estimates of incidence and mortality worldwide for 36 cancers in 185 countries, CA A Cancer J. Clin. 71 (2021) 209–249, https://doi.org/10.3322/caac.21660.

[2] Y.K. Kang, N. Boku, T. Satoh, M.H. Ryu, Y. Chao, K. Kato, H.C. Chung, J.S. Chen, K. Muro, W.K. Kang, K.H. Yeh, T. Yoshikawa, S.C. Oh, L.Y. Bai, T. Tamura, K. W. Lee, Y. Hamamoto, J.G. Kim, K. Chin, D.Y. Oh, K. Minashi, J.Y. Cho, M. Tsuda, L.T. Chen, Nivolumab in patients with advanced gastric or gastro-oesophageal junction cancer refractory to, or intolerant of, at least two previous chemotherapy regimens (ONO-4538-12, ATTRACTION-2): a randomised, double-blind, placebo-controlled, phase 3 trial, Lancet 390 (2017) 2461–2471, https://doi.org/10.1016/s0140-6736(17)31827-5.

[3] C.S. Fuchs, T. Doi, R.W. Jang, K. Muro, T. Satoh, M. Machado, W. Sun, S.I. Jalal, M. A. Shah, J.P. Metges, M. Garrido, T. Golan, M. Mandala, Z.A. Wainberg, D. V. Catenacci, A. Ohtsu, K. Shitara, R. Geva, J. Bleeker, A.H. Ko, G. Ku, P. Philip, P. C. Enzinger, Y.J. Bang, D. Levitan, J. Wang, M. Rosales, R.P. Dalal, H.H. Yoon, Safety and efficacy of pembrolizumab monotherapy in patients with previously treated advanced gastric and gastroesophageal junction cancer: phase 2 clinical KEYNOTE-059 trial, JAMA Oncol 4 (2018), e180013, https://doi.org/10.1001/jamaoncol.2018.0013.

[4] K. Shitara, M. Ozguroglu, Y.J. Bang, M. Di Bartolomeo, M. Mandala, M.H. Ryu, L. Fornaro, T. Olesinski, C. Caglevic, H.C. Chung, K. Muro, E. Goekkurt, W. Mansoor, R.S. McDermott, E. Shacham-Shmueli, X. Chen, C. Mayo, S.P. Kang, A. Ohtsu, C.S. Fuchs, Pembrolizumab versus paclitaxel for previously treated, advanced gastric or gastro-oesophageal junction cancer (KEYNOTE-061): a randomised, open-label, controlled, phase 3 trial, Lancet 392 (2018) 123–133, https://doi.org/10.1016/s0140-6736(18)31257-1.

[5] K. Shitara, E. Van Cutsem, Y.J. Bang, C. Fuchs, L. Wyrwicz, K.W. Lee, I. Kudaba, M. Garrido, H.C. Chung, J. Lee, H.R. Castro, W. Mansoor, M.I. Braghiroli, N. Karaseva, C. Caglevic, L. Villanueva, E. Goekkurt, H. Satake, P. Enzinger, M. Alsina, A. Benson, J. Chao, A.H. Ko, Z.A. Wainberg, U. Kher, S. Shah, S.P. Kang, J. Tabernero, Efficacy and safety of pembrolizumab or pembrolizumab plus chemotherapy vs chemotherapy alone for patients with first-line, advanced gastric cancer: the KEYNOTE-062 phase 3 randomized clinical trial, JAMA Oncol 6 (2020) 1571–1580, https://doi.org/10.1001/jamaoncol.2020.3370.

[6] TCGA, Comprehensive molecular characterization of gastric adenocarcinoma, Nature 513 (2014) 202–209, https://doi.org/10.1038/nature13480.

[7] R. Cristescu, J. Lee, M. Nebozhyn, K.M. Kim, J.C. Ting, S.S. Wong, J. Liu, Y.G. Yue, J. Wang, K. Yu, X.S. Ye, I.G. Do, S. Liu, L. Gong, J. Fu, J.G. Jin, M.G. Choi, T. S. Sohn, J.H. Lee, J.M. Bae, S.T. Kim, S.H. Park, I. Sohn, S.H. Jung, P. Tan, R. Chen, J. Hardwick, W.K. Kang, M. Ayers, D. Hongyue, C. Reinhard, A. Loboda, S. Kim, A. Aggarwal, Molecular analysis of gastric cancer identifies subtypes associated with distinct clinical outcomes, Nat. Med. 21 (2015) 449–456, https://doi.org/10.1038/nm.3850.

[8] X. Han, H. Lu, X. Tang, Y. Zhao, H. Liu, Immunogenomic characterization in gastric cancer identifies microenvironmental and immunotherapeutically relevant gene signatures, Immun Inflamm Dis (2021), https://doi.org/10.1002/iid3.539.

[9] Y. Lin, X. Pan, L. Zhao, C. Yang, Z. Zhang, B. Wang, Z. Gao, K. Jiang, Y. Ye, S. Wang, Z. Shen, Immune cell infiltration signatures identified molecular subtypes and underlying mechanisms in gastric cancer, NPJ Genom Med 6 (2021) 83, https://doi.org/10.1038/s41525-021-00249-x.

[10] Y. Sato, I. Wada, K. Odaira, A. Hosoi, Y. Kobayashi, K. Nagaoka, T. Karasaki, H. Matsushita, K. Yagi, H. Yamashita, M. Fujita, S. Watanabe, T. Kamatani, F. Miya, J. Mineno, H. Nakagawa, T. Tsunoda, S. Takahashi, Y. Seto, K. Kakimi, Integrative immunogenomic analysis of gastric cancer dictates novel immunological classification and the functional status of tumor-infiltrating cells, Clin Transl Immunology 9 (2020) e1194, https://doi.org/10.1002/cti2.1194.

[11] D.S. Chen, I. Mellman, Oncology meets immunology: the cancer-immunity cycle, Immunity 39 (2013) 1–10, https://doi.org/10.1016/j.immuni.2013.07.012.

[12] M.I. Love, W. Huber, S. Anders, Moderated estimation of fold change and dispersion for RNA-seq data with DESeq2, Genome Biol. 15 (2014) 550, https://doi.org/10.1186/s13059-014-0550-8.

[13] R.J. Kishton, M. Sukumar, N.P. Restifo, Metabolic regulation of T cell longevity and function in tumor immunotherapy, Cell Metabol. 26 (2017) 94–109, https://doi.org/10.1016/j.cmet.2017.06.016.

[14] S. Eikawa, M. Nishida, S. Mizukami, C. Yamazaki, E. Nakayama, H. Udono, Immune-mediated antitumor effect by type 2 diabetes drug, metformin, Proc. Natl. Acad. Sci. U.S.A. 112 (2015) 1809–1814, https://doi.org/10.1073/pnas.1417636112.

[15] J.R. Molina, Y. Sun, M. Protopopova, S. Gera, M. Bandi, C. Bristow, T. McAfoos, P. Morlacchi, J. Ackroyd, A.A. Agip, G. Al-Atrash, J. Asara, J. Bardenhagen, C. C. Carrillo, C. Carroll, E. Chang, S. Ciurea, J.B. Cross, B. Czako, A. Deem, N. Daver, J.F. de Groot, J.W. Dong, N. Feng, G. Gao, J. Gay, M.G. Do, J. Greer, V. Giuliani, J. Han, L. Han, V.K. Henry, J. Hirst, S. Huang, Y. Jiang, Z. Kang, T. Khor, S. Konoplev, Y.H. Lin, G. Liu, A. Lodi, T. Lofton, H. Ma, M. Mahendra, P. Matre, R. Mullinax, M. Peoples, A. Petrocchi, J. Rodriguez-Canale, R. Serreli, T. Shi, M. Smith, Y. Tabe, J. Theroff, S. Tiziani, Q. Xu, Q. Zhang, F. Muller, R.A. DePinho, C. Toniatti, G.F. Draetta, T.P. Heffernan, M. Konopleva, P. Jones, M.E. Di Francesco, J.R. Marszalek, An inhibitor of oxidative phosphorylation exploits cancer vulnerability, Nat. Med. 24 (2018) 1036–1046, https://doi.org/10.1038/s41591-018-0052-4.

[16] M. Nishida, N. Yamashita, T. Ogawa, K. Koseki, E. Warabi, T. Ohue, M. Komatsu, H. Matsushita, K. Kakimi, E. Kawakami, K. Shiroguchi, H. Udono, Mitochondrial reactive oxygen species trigger metformin-dependent antitumor immunity via activation of Nrf2/mTORC1/p62 axis in tumor-infiltrating CD8T lymphocytes, J Immunother Cancer 9 (2021), https://doi.org/10.1136/jitc-2021-002954.

[17] J. Yang, S.A. Mani, J.L. Donaher, S. Ramaswamy, R.A. Itzykson, C. Come, P. Savagner, I. Gitelman, A. Richardson, R.A. Weinberg, Twist, a master regulator of morphogenesis, plays an essential role in tumor metastasis, Cell 117 (2004) 927–939, https://doi.org/10.1016/j.cell.2004.06.006.

[18] T.T. Onder, P.B. Gupta, S.A. Mani, J. Yang, E.S. Lander, R.A. Weinberg, Loss of E-cadherin promotes metastasis via multiple downstream transcriptional pathways, Cancer Res. 68 (2008) 3645–3654, https://doi.org/10.1158/0008-5472.Can-07-2938.

[19] H. Zhao, H. Hu, B. Chen, W. Xu, J. Zhao, C. Huang, Y. Xing, H. Lv, C. Nie, J. Wang, Y. He, S.Q. Wang, X.B. Chen, Overview on the role of E-cadherin in gastric cancer: dysregulation and clinical implications, Front Mol Biosci 8 (2021), 689139, https://doi.org/10.3389/fmolb.2021.689139.

[20] V. Padmanaban, I. Krol, Y. Suhail, B.M. Szczerba, N. Aceto, J.S. Bader, A.J. Ewald, E-cadherin is required for metastasis in multiple models of breast cancer, Nature 573 (2019) 439–444, https://doi.org/10.1038/s41586-019-1526-3.

[21] F. Finotello, D. Rieder, H. Hackl, Z. Trajanoski, Next-generation computational tools for interrogating cancer immunity, Nat. Rev. Genet. 20 (2019) 724–746, https://doi.org/10.1038/s41576-019-0166-7.